NIH Public Access
Author Manuscript
Circ Res. Author manuscript; available in PMC 2012 September 2.

Published in final edited form as:
Circ Res. 2011 September 2; 109(6): 658–669. doi:10.1161/CIRCRESAHA.111.248260.

Haploinsufficiency of Target of Rapamycin Attenuates Cardiomyopathies in Adult Zebrafish

Yonghe Ding, **Xiaojing Sun**[*], **Wei Huang**[*], **Tiffany Hoage**, **Margaret Redfield**, **Sudhir Kushwaha**, **Sridhar Sivasubbu**, **Xueying Lin**, **Stephen Ekker**, and **Xiaolei Xu**
Department of Biochemistry and Molecular Biology, Mayo Clinic College of Medicine, Rochester, MN 55905 (Y.D., X.S., W.H., T.H., X.L., S.E., X.X.); Division of Cardiovascular Diseases, Department of Medicine, Mayo Clinic College of Medicine, Rochester, MN 55905 (Y.D., X.S., W.H., T.H., M.R., S.K., X.L., X.X.); Department of Surgery, Johns Hopkins University School of Medicine, Baltimore, MD 21205 (W.H. present address); Institute of Genomics and Integrative Biology, Council of Scientific and Industrial Research, Mall Road, Delhi 110007, India (S.S.)

Abstract

Rationale—Although a cardioprotective function of target of rapamycin (TOR) signaling inhibition has been suggested by pharmacological studies using rapamycin, genetic evidences are still lacking. Here, we explored adult zebrafish as a novel vertebrate model for dissecting signaling pathways in cardiomyopathy.

Objective—We generate the second adult zebrafish cardiomyopathy model induced by doxorubicin (DOX). By genetically analyzing both the DOX and our previous established anemia-induced cardiomyopathy models, we aim to decipher the functions of TOR signaling in cardiomyopathies of different etiology.

Methods and Results—Along the progression of both cardiomyopathy models, we detected dynamic TOR activity at different stages of pathogenesis as well as distinct effects of TOR signaling inhibition. Nevertheless, cardiac enlargement in both models can be effectively attenuated by inhibition of TOR signaling via short-term rapamycin treatment. To assess the long term effects of TOR reduction, we utilized a *zebrafish target of rapamycin (ztor)* mutant identified from an insertional mutagenesis screen. We show that TOR haploinsufficiency in the *ztor* heterozygous fish improved cardiac function, prevented pathological remodeling events, and ultimately reduced mortality in both adult fish models of cardiomyopathy. Mechanistically, these cardioprotective effects are conveyed by the anti-hypertrophy, anti-apoptosis, and proautophagy function of TOR signaling inhibition.

Conclusions—Our results prove adult zebrafish as a conserved novel vertebrate model for human cardiomyopathies. Moreover, we provide the first genetic evidence to demonstrate a long-term cardioprotective effect of TOR signaling inhibition on at least two cardiomyopathies of distinct etiology, despite dynamic TOR activities during their pathogenesis.

Correspondence to Xiaolei Xu, Ph.D., Department of Biochemistry and Molecular Biology, Mayo Clinic College of Medicine, 200 First Street SW, Rochester, MN 55905. Tel.: 1-507-284-0685; Fax: 1-507-538-6418; xu.xiaolei@mayo.edu.
[*]contributed equally

DISCLOSURES None

Publisher's Disclaimer: This is a PDF file of an unedited manuscript that has been accepted for publication. As a service to our customers we are providing this early version of the manuscript. The manuscript will undergo copyediting, typesetting, and review of the resulting proof before it is published in its final citable form. Please note that during the production process errors may be discovered which could affect the content, and all legal disclaimers that apply to the journal pertain.

NIH-PA Author Manuscript
NIH-PA Author Manuscript
NIH-PA Author Manuscript

NIH-PA Author Manuscript

NIH-PA Author Manuscript

NIH-PA Author Manuscript

Keywords

doxorubicin; cardiotoxicity; cardiomyopathy; target of rapamycin; zebrafish; anemia

INTRODUCTION

Due to its advantageous embryology and unique genetic tools, zebrafish embryo has become a recognized vertebrate model for studying genetic aspects of human diseases.[1] However, many human diseases, such as cardiomyopathy and heart failure, are adult diseases with a progressive pathogenesis, which are difficult to be recapitulated in zebrafish embryos. To explore the potential of adult zebrafish for cardiomyopathy studies, we have developed the first adult zebrafish model for cardiomyopathy induced by anemia.[2] We characterized pathogenesis in the heart of *tr265*, an anemic mutant incurred by a Band 3 mutation in erythocytes that was identified from an ENU mutagenesis screen.[3] The chronic anemic stress to the heart induces profound cardiac enlargement, followed by cardiomyopathy-like phenotypes.[2] Due to the unique regeneration capacity of a zebrafish heart, both cardiomyocyte (CM) hypertrophy and hyperplasia contribute to the pathogenesis in the *tr265* fish. To validate adult zebrafish as a conserved vertebrate model for cardiac diseases, its cardiac responses to other cardiomyopathy-inducing biomechanical stresses need to be assessed.

In the present study, we report the second adult zebrafish model of cardiomyopathy induced by Doxorubicin (DOX, adriamycin). In contrast to the anemia model, we found that CM hyperplasia does not contribute to this type of cardiomyopathy. DOX is an anthracyclin drug that has been used in the treatment of a broad spectrum of cancers. However, overdose of DOX impose toxicities on the heart,[4] which can be categorized into two different types.[5,6] Acute cardiotoxicity occurs immediately after the administration of DOX, presenting as hypotension, transient cardiac rhythm disturbance, or reduced heart size. By contrast, chronic cardiotoxicity appears years or decades after patient exposure to DOX, typically presenting as an irreversible, cumulative, and dose-dependent cardiomyopathy that finally leads to congestive heart failure.[5,6] Mechanistically, it has been hypothesized that DOX-induced cardiotoxicity is mediated by activation of free radicals-induced mitochondrial damage, which in turn imposes oxidative stress on the heart and triggers apoptotic cardiomyocyte death.[7,8]

One of the major goals of cardiomyopathy studies is to identify a common pathological signaling pathway that can be intervened to achieve therapeutic benefit. Target of rapamycin (TOR) pathway is one of the candidates that interprets a variety of inputs, including nutritional status, energy level, growth factors, as well as cellular stresses, and then coordinates the regulation of cell growth, cell proliferation, and cell death.[9] A cardioprotective function of TOR signaling inhibition has been suggested by pharmacological studies using rapamycin, a specific inhibitor of TOR. In mice, rapamycin prevents cardiac hypertrophy induced by aortic constriction,[10,11] by thyroid hormone,[12] or in the LEOPARD syndrome.[13] In humans, the treatment of patients following cardiac transplantation with rapamycin significantly attenuates left ventricular hypertrophy.[14] However, this notion based on pharmacological studies has not been supported by direct genetic analysis of components in TOR signaling.[15]

In this study, we first set up a DOX-induced cardiomyopathy model in adult zebrafish. We then sought to utilize the *zebrafish target of rapamycin* mutant (ztor), which we have isolated from an insertional mutagenesis screen, to elucidate functions of TOR signaling in both DOX and our previously established anemia-induced cardiomyopathy models. Our data

NIH-PA Author Manuscript

NIH-PA Author Manuscript

NIH-PA Author Manuscript

uncovered dynamic activity of TOR signaling in pathogenesis of cardiomyopathies and provides the first genetic evidence to support that TOR signaling is a common pathological pathway that can be leveraged for therapeutic benefits for cardiomyopathies of different etiology.

METHODS

An expanded material and methods section is available in the online data supplement at http://circres.ahajournals.org.

Cardiomyocyte dissociation and primary cardiomyocyte culture

Cardiomyocytes (CMs) from dissected ventricles of *Tg(cmlc2:nuDsRed)* fish or *tr265* fish were dissociated as described previously.[2] The newly dissociated CMs usually attached to the cell culture chamber within 1 h, which allows us to capture images for CMs area measurement by outlining each individual CM using ImageJ software (NIH).[2] The CM identity was determined by either the nuDsRed reporter in the *Tg(cmlc2:nuDsRed)* transgenic fish, Mef2, or α-actinin antibody staining. Both rod- and round-shape CM population were noted during the primary CM culture. Twenty to forty rod-shape CMs were identified for size quantification.

Cardiac functional analysis in adult fish

For shortening fraction (FS) measuring, *casper;Tg(cmlc2:nuDsRed)* fish were anesthetized in 0.16 mg/mL tricaine for 2.5 min and placed ventral side up on a slotted sponge. Movies of beating hearts were recorded using a digital camera attached to a fluorescent Leica MZ FLI III microscope. Images from movies were then used to measure the axis length between the myocardial borders of the ventricles at diastole and systole, respectively (see Supplemental Fig. 2). The percent fraction shortening (FS%) was calculated using the formula FS% = (length at diastole – length at systole)/(length at diastole) × 100. The red blood cell flow rate was measured as described previously.[2] More than 6 fish were used for each experimental group.

Transposon-mediated insertional mutagenesis screen

The gene-breaking transposon P9 was generated by subcloning the SB-P6 GBT[16] into a nearly full-length Tol2 vector.[17] Incrosses were conducted for each founder fish family to identify families exhibiting embryonic lethal phenotypes. *xu015* is one of the 41 embryonic-lethal mutants identified from this screen.

Statistics

All values are shown as mean ± standard error (SEM, n≥3 otherwise noted). Student's *t*-test was used for comparisons between special two groups and ANOVA was used for assessment differences among three or more groups. *P*-values for the analysis of survival rates were determined by log-rank test. A $P<0.05$ was considered significant.

RESULTS

DOX induces progressive and pathological cardiomyopathy in adult zebrafish

To assess DOX-induced cardiac responses in adult zebrafish, we injected DOX intraperitoneally into *casper* fish ages from two months to one-year old. The *casper* fish was chosen due to its transparent body at adult stage which facilitates both DOX injection and cardiac function measurement.[18] Based on mice studies,[19,20] we empirically determined the proper dose. Injection of 50 μg/gram body mass (gbm) DOX led to severe mortality, as well

NIH-PA Author Manuscript

NIH-PA Author Manuscript

NIH-PA Author Manuscript

as significant loss of body and heart mass at 4 weeks post-injection, although the heart surface area/body weight index remained unchanged (Figure1A, 1B and Online Figure I). In contrast, injection of 20 μg/gbm DOX bypasses the severe mortality. Most fish survived this dose without a detectable change in body shape/size. However, a significantly enlarged heart was detected at both 4 weeks and thereafter, such as 12 weeks post-injection (Figure 1A, 1B and Online Figure I). To assess whether the enlarged heart is due to myocyte hypertrophy, we dissociated individual hearts and isolated single cardiomyocytes (CMs), whose identity was indicated by either α-actinin or Mef2 antibody staining (Figure 1C). Averages size of individual cardiomyocytes was significantly enlarged (Figure 1C and 1D). The width but not the length of individual cardiomyocytes was increased (Figure 1E and 1F), confirming a hypertrophic growth.

Due to its small size, a beating zebrafish heart has been difficult to be documented by echocardiography-based imaging technology.[21] We developed an alternative approach by crossing the semi-transparent *casper* with the *Tg(cmlc2:nuDsRed)* line, which fluorescently labels all cardiomyocyte nuclei red.[22] The resulted *casper; Tg(cmlc2:nuDsRed)* fish line allows the documentation of a beating heart using a fluorescent microscope directly. The recorded movies were then used to calculate fraction shortening and heart rate (Online Figure IIA). We detected reduced fraction shortening starting at 4 weeks post-injection (Figure 1G), but unchanged heart rate (Online Figure IIC). To validate the cardiac function study, we further quantified red blood cell (RBC) flow rate, an assay developed to reflect cardiac function indirectly.[2] We detected a reduction of RBC flow rate in the DOX-treated fish beginning at 4 weeks post-injection (Online Figure IIB).

We then examined hallmarks of pathological cardiomyopathy in the DOX-injected fish. Expression of the *atrial natriuretic factor (anf)*, a fetal gene and molecular marker of cardiomyocyte hypertrophy, was significantly upregulated post-DOX injection (Figure 1H). Muscular disarray and myofibril loss were detected at 12 weeks post-DOX injection via either α-actinin antibody staining or transmission electronic microscopy (Figure 1I and 1J). Together, these data suggest that DOX induces progressive and pathological cardiomyopathy in adult zebrafish. The progression from adaptation phase to decompensation phase occurs at around week 4 post-injection, which continues to progress into more severe cardiomyopathy at later stages.

Dynamics of TOR signaling during pathogenesis of two adult zebrafish models of cardiomyopathy

To assess the role of TOR signaling in DOX-induced cardiac responses, we measured the level of pS6K, an essential downstream signaling axe of TOR. We did not detect significant changes of pS6K level at 3 days post-DOX injection. In contrast, pS6K level was consistently higher than that in the control group at both week 4 and 12 post-injection, while the total protein level of S6K remained unchanged (Figure 2A).

We also measured pS6K level in our previously established *tr265* anemia model. Our previous studies of this model revealed cardiomyocyte hypertrophy at the 3–10 weeks old *tr265* fish. However, a small portion of the *tr265* fish survived to week 12–16 are characterized by heart enlargement consisting of increased number of cardiomyocytes with smaller size.[2] Consistent to the notion that *tr265* fish at week-6 and week-12 age represent two types of cardiac enlargement with different cellular nature, we detected upregulated pS6K at week 6 but downregulated pS6K level at week 12 (Figure 2B). Together, our data suggested dynamic TOR activity along the pathogenesis of two cardiomyopathy models.

NIH-PA Author Manuscript

NIH-PA Author Manuscript

NIH-PA Author Manuscript

Temporal TOR reduction via rapamycin treatment attenuates cardiac enlargement induced by either DOX or anemia

Next, we assess the effect of rapamycin treatment on different models of cardiomyopathy. Firstly, we found that rapamycin treatment can effectively reduce pS6K level in both the DOX and anemia models (Figure 2A and 2B). Secondly, we detected that one-week rapamycin treatment effectively attenuated DOX-induced cardiac enlargement at both week 4 and week 12 post-injection (Figure 2C and 2D). Similarity, we also found that the heart enlargement was significantly attenuated by rapamycin treatment at both week 4 and week 7, but not week 12-old *tr265* fish (Figure 2E), while the rapamycin treatment itself doesn't affect the general fish growth (data not shown). This line of data support the notion that cardiac enlargement at week 12 is due to a distinct molecular/cellular mechanism. To further validate this notion and to exclude the possibility that distinct effects of rapamycin are simply due to different ages of fish, we utilized another anemia model induced by phenylhydrazine (PHZ), a compound that can be used to induce anemia in adult fish at any age.[2] We firstly validate that a three-week PHZ treatment induced heart enlargement in fish at both week 3–5 and week 10–12 time window (Figure 2F). We further detected that one week rapamycin co-treatment effectively attenuated the PHZ-induced heart enlargement in both fish groups, without disturbing the body length (Figure 2F and data not shown). This observation validated the notion that 11–12 week-old *tr265* fish represents a unique pathologic stage that is characterized by reduced cardiomyocyte size and reduced TOR signaling. Together, our data demonstrated a conserved function of rapamycin in attenuating cardiac enlargement in zebrafish models of cardiomyopathies, as has been previously shown in mammalian models and humans.

Sustained TOR reduction via *ztor*$^{+/-}$ attenuates cardiomyopathy induced by either anemia or DOX

We have conducted an insertional mutagenic screen using P9, a Tol2-based transposon vector containing a gene-breaking cassette, and identified *xu015*, a recessive embryonic lethal zebrafish mutant (Online Figure IIIA).[16] Through linker-mediated PCR (LM-PCR), a P9 insertion was detected in the intron between exon 5 and exon 6 of the *zebrafish target of rapamycin (ztor)* gene (Figure 3A). The linkage between this P9 insertion and the *xu015* mutant phenotypes was established by genotyping 20 *xu015/xu015* embryos (LOD score >6, Online Figure IIIB). It was predicted that the insertion of P9 into an intron would hijack the splicing machinery of the target gene and lead to generation of two end transcripts, a N-terminal cDNA consisting of the first five exons and a C-terminal cDNA that fused with the GFP in the Tol2 construct.[16] Indeed, both end products can be detected by RT-PCR (Online Figure IIIC). The mRNA level of *ztor* was reduced in *xu015* mutant to around 11% of that in normal sibling (Figure 3C). The TOR protein level was also reduced, as well as the phosphorylation level of ribosomal S6K, while the total S6K level remained unchanged (Figure 3D). Based on the above evidence, we conclude that *xu015* is a *ztor* hypomorphic zebrafish mutant. In the following text, we will refer to this homozygous mutant as *ztor*$^{-/-}$and heterozygous mutant as *ztor*$^{+/-}$.

The *ztor*$^{-/-}$ embryos appeared normal until 6 days post-fertilization (dpf), when the larvae became less active and exhibited characteristic dark livers at 7 dpf (Figure 3B). Most of the embryos died at 10 dpf. The size of *ztor*$^{-/-}$ embryonic heart appeared smaller at diastole but not systole (Online Figure IIID). Both significantly reduced cardiomyocyte proliferation and cell size was observed in the *ztor*$^{-/-}$ embryonic heart at 7 dpf, as revealed by immunostaining with antibodies against PCNA and β-catenin (Figure 3E through 3H). However, the *ztor*$^{+/-}$ fish exhibited no overt phenotype until at least 9-months old age, as evidenced by their normal body length and body weight (data not shown). The TOR protein level, however, is reduced by 35% in the *ztor*$^{+/-}$ fish at 6-months old. Both pS6K

NIH-PA Author Manuscript

NIH-PA Author Manuscript

NIH-PA Author Manuscript

phosphorylation level and pAKT(Ser473) are reduced (Figure 3I), indicating that both TORC1 and TORC2 are affected. Similar changes of TOR downstream branches were detected in fish treated with 0.2 μmol/L rapamycin 12 h daily for consecutive 7 days. However, fish treated with 0.4 μmol/L rapamycin 4 h daily for 7 consecutive days exhibits reduced pS6K but activated pAKT(ser473), which is consistent to the existence of a negative feedback regulation by TORC1 to PI3K-AKT signaling.[9] Consistent to the notion that 4E-BP1 is a negative downstream effector of TOR signaling, we detected upregulated p4E-BP1 level in adult *ztor*$^{+/-}$ fish compared to that in wild-type fish (Figure 3I).

The generation of *ztor*$^{+/-}$ fish provides an opportunity to study the long-term effect of TOR haploinsufficiency on adult fish models of cardiomyopathy. To assess effects of sustained TOR reduction on DOX-induced cardiomyopathy, we injected 20 μg/gbm DOX into two-month old *ztor*$^{+/-}$ fish. Compared to wild type control, the recovery of myofibril organization was detected in *ztor*$^{+/-}$ at late stages, which is characterized by more evenly distributed expression of α-actinin, improved lateral alignment and organization of sarcomeres (Figure 4A and 4B). Both ventricular enlargement and fetal gene *anf* re-activation were significantly rescued at 8 weeks post-injection (Figure 4C and 4D). The RBC flow rate, an indirect index of cardiac function, was better maintained in *ztor*$^{+/-}$ fish at week 8 post-DOX injection and thereafter (Figure 4E). However, it is worthy pointing out that, while this indirect assay is useful when direct quantification of fractional shortening cannot be conducted in a non-transparent adult fish, it cannot replace fractional shortening studies to assess cardiac function. More importantly, the survival rate was significantly increased in *ztor*$^{+/-}$ fish after DOX treatment compared to that in wild-type control fish (Figure 4F).

We also assessed the long-term effect of TOR haploinsufficiency on the anemia model by generating a *tr265; ztor*$^{+/-}$ double mutant fish line. Similar to the DOX model, the enlarged heart size in *tr265* was attenuated in the *tr265; ztor*$^{+/-}$ double mutant fish, as quantified by the ratio of ventricular size to body length index at 4-week old age (Online Figure IVA and IVB). In addition, an elevated RBC flow rate was observed, indicating an improved cardiac function (Online Figure IVC). We went on to examine other hallmarks of cardiomyopathy and found that the expression level of *anf* was significantly reduced in the *tr265; ztor*$^{+/-}$ double mutant fish (Online Figure IVD), as well as reduced muscular disarray and myofibril loss (Online Figure IVF-IVI). Importantly, the survival rate was also significantly improved in the *tr265; ztor*$^{+/-}$ double mutants than that in *tr265* fish (Figure 4G). As a control, we detected no difference in the relative hemoglobin concentration at week 9 between *tr265; ztor*$^{+/-}$ and *tr265* fish (Online Figure IVE), suggesting that *ztor* haploinsufficiency did not restore hemoglobin level in anemic fish. Furthermore, we validated that *ztor*$^{+/-}$ fish exhibited attenuated cardiac enlargement induced by PHZ (Online Figure VIA through VIC). Together, the above data demonstrated that the suppression of TOR signaling exerts cardioprotective effects in both zebrafish models of cardiomyopathies.

Functions of TOR signaling inhibition on cardiomyocyte hypertrophy

To elucidate the cellular mechanisms for the cardioprotective functions of TOR signaling inhibition, we first assessed cardiomyocyte hypertrophy. We found that the cardiomyocyte enlargement induced by DOX injection in the wild type fish was significantly attenuated in *the ztor*$^{+/-}$ fish (Figure 5A). Similarly, the size of isolated cardiomyocytes was reduced in *tr265; ztor*$^{+/-}$ double mutants compared to that in the *tr265* fish at 4 weeks old (Figure 5B).

To test the hypothesis that the anti-cardiomyocyte hypertrophy function of TOR signaling inhibition is due to its direct action on cardiomyocytes, we exploited zebrafish primary cardiomyocyte culture system. Immediately after dissociation and culture, we noticed rod-shaped cells whose geometry resembles typical cardiomyocytes in mammals (Online Figure

NIH-PA Author Manuscript

NIH-PA Author Manuscript

NIH-PA Author Manuscript

VA). These cardiomyocytes usually attached to the cell culture chamber within 1 hour and changed their shape after 3 days in culture, appearing to be more spread-out with multiple filopodia (for a similar observation, see[23]), suggesting a de-differentiation process of the cardiomyocytes. The sarcomere structures can be detected by either differential interference contrast (DIC) imaging or α-actinin staining (Online Figure VA and VB). The averaged cardiomyocytes size remained mostly unchanged throughout the 7-day culture process, despite the change of cell shape (Online Figure VC). Treatment with DOX for 2 hours at day 1 induced enlargement of cardiomyocytes at day 5 in a dose-dependent fashion (Online Figure VIIB). This observation indicated that adult zebrafish cardiomyocytes exhibits a conserved hypertrophic response in mammals.[24,25] Consistent to our *in vivo* studies, co-treatment with rapamycin effectively attenuated cardiomyocyte hypertrophy induced by DOX *in vitro* (Figure 5C and 5D).

Functions of TOR inhibition on myocyte proliferation

In addition to myocyte hypertrophy (increased cell size), a zebrafish heart may respond to extrinsic or intrinsic stresses by changing cardiomyocyte cell number via cell proliferation or cell death.[26] In the *tr265* anemia model, we found that myocyte hyperplasia contributed to all stages of pathogenesis.[2] Therefore, we assessed myocyte proliferation in the DOX model via PCNA staining of sectioned ventricles. The identity of cardiomyocytes was indicated by co-staining with a Mef2 antibody. We found that the cardiomyocytes PCNA index remained unchanged at either 3 days or 4 weeks post-DOX injection (Figure 6A and 6C). There is also no significant PCNA index change detected in the *ztor*$^{+/-}$ fish injected with or without DOX (Figure 6D). Similarly, we found that the proliferation index in the DOX-induced cellular hypertrophy model, as represented by BrdU incorporation, also remains unchanged (Figure 6B and 6E). Together, we conclude that, in contrast to the *tr265* model, myocyte hyperplasia does not contribute to the enlarged heart seen in the DOX model.

Consistent with an anti-proliferation function of TOR signaling inhibition in cancer cells, such function has also been noted in zebrafish cardiomyocytes. In the DOX model, we found that rapamycin treatment inhibits cardiomyocyte proliferation, either in the presence or absence of DOX (Figure 6D and 6E). Similarly in the *tr265* anemia model of cardiomyopathy, increased proliferation was significantly attenuated by rapamycin treatment or in *tr265; ztor*$^{+/-}$ fish (Figure 6F–6G). The similar observation was also made in the anemic model induced by PHZ (Online Figure VID). To validate that the anti-proliferative function of TOR signaling inhibition is due to a direct action on cardiomyocytes, we measured the BrdU index of cardiomyocytes *in vitro*. Consistently, we found that BrdU index in cardiomyocytes isolated from the *tr265* fish were significantly reduced upon rapamycin treatment (Figure 6E and 6H). Of note, this anti-proliferation function of rapamycin on cardiomyocytes was also detected in wild type siblings both *in vivo* and *in vitro* (Figure 6D, 6E, 6G and 6H).

Functions of TOR inhibition on cardiomyocyte apoptosis and autophagy

Previous studies indicated that cardiomyocyte apoptosis contributes significantly to DOX induced cardiotoxicity,[27,28] but not to the *tr265* model of cardiomyopathy induced by anemia.[2] Therefore, we focused on the DOX model and assessed the contribution of cardiomyocyte apoptosis during DOX-induced cardiomyopathy, as well as the effects of TOR signaling inhibition. We found out that apoptosis index was dramatically induced at 4 weeks, but not 3 days post-DOX injection (20 μg/gbm) (Figure 7A, 7C and 7D), suggesting its contribution to DOX-induced late onset cardiomyopathy. In our *in vitro* cardiomyocyte culture system, we also observed a dose-dependent enlargement of cardiomyocyte size, as well as activated apoptosis and increased cardiomyocyte loss (Online Figure VIIA and

NIH-PA Author Manuscript

NIH-PA Author Manuscript

NIH-PA Author Manuscript

VIIC). Reduction of TOR signaling via either *ztor*$^{+/-}$ or one-week rapamycin treatment effectively reduced the activated cardiomyocyte apoptosis *in vivo* (Figure 7A, 7C and 7D). Consistently, the apoptotic signal was also significantly attenuated after co-treatment with rapamycin *in vitro* (Figure 7B and 7E). Together, our data indicated an anti-apoptotic function for TOR signaling inhibition.

Prompted by the implication of autophagy in cardiomyopathies and DOX-induced cardiotoxicity,[29–31] we assessed functions of autophagy in DOX-induced cardiomyopathy model. In contrast to pS6K that is positively regulated by TOR, autophagy is a cellular degradation pathway that is negatively regulated by TOR. Lc3 II (microtubule-associated protein light chain 3 form 2) and p62/SQSTEM1 are two molecular markers that have been widely used to assess autophagic flux.[32,33] The levels of Lc3 II are proportional to the number of accumulated autophagic vacuoles, while the level of p62 protein, which is degraded by autophagy, is inversely related to autophagy activity. We detected activated autophagy at early stages after DOX-injection, but suppressed autophagy at later stages, as indicated by western blot to reveal both the Lc3 II conversion and p62 degradation (Figure 8A). This observation was validated by quantifying Lc3 aggregation dots after injecting DOX into *Tg(GFP-Lc3)* transgenic fish (Figures 8B and 8C).[32] Rapamycin treatment restored autophagy to a level that is comparable to that in wild type at 12 weeks post-injection (Figure 8C). Together, our data confirmed dynamic activity of autophagy at different stages of pathogenesis in DOX-induced cardiomyopathy, while depressed autophagy reflects the later decompensational hypertrophy stage. Therefore, we propose that the pro-autophagy function of TOR inhibition might also be accountable for its cardioprotective effects.

Distinct functions of TOR signaling inhibition between DOX-induced acute cardiotoxicity and late-onset cardiomyopathy

Our data in zebrafish suggest a beneficial effect of TOR inhibition/autophagy activation on DOX-induced cardiomyopathy. However, two recent studies in rodent models indicated either a detrimental effect of TOR inhibition or a protective effect of TOR activation on DOX-induced acute cardiotoxicity.[19,29] Prompted by the observation that autophagy activity is opposite at early stages vs. later stages after DOX-injection, we hypothesized that these seemingly conflicting conclusions resulted from stage-dependent functions of TOR. To test this hypothesis, we assessed adult fish injected with a higher dose of DOX (50 ug/gbm) to exaggerate its acute cardiotoxicity, which is characterized by reduced heart size and severe mortality. Similar to fish injected with low dose of DOX (20 ug/gbm), activated autophagy and unchanged p-S6K levels were detected in fish at 3 days post high-dose DOX-injection. Co-treatment with rapamycin further enhanced the autophagy activity, and abolished most of the p-S6K level in both groups, while had no significant impact on the level of total S6K protein (Online Figure VIIIA). Indeed, in addition to opposite autophagy activities, the following two observations further validate the stage-dependent functions of TOR signaling inhibition. First, in contrast to an anti-apoptosis function during late-onset cardiomyopathy, rapamycin co-treatment increased the cardiomyocyte apoptosis index in high-dose DOX-induced acute cardiotoxicity (Online Figure VIIIC and VIIID). Secondly, rather than a cardioprotective effect in fish cardiomyopathy models but similar to those in acute rodent cardiotoxicity models, co-treatment of rapamycin further exerted a deleterious effect on the high dose DOX-induced acute cardiotoxicity in zebrafish, as indicated by a further increased fish mortality (Online Figure VIIIB). Together, our data strongly suggested that TOR signaling inhibition exerts opposite effects on DOX-induced acute cardiotoxicity and late-onset cardiomyopathy.

NIH-PA Author Manuscript

NIH-PA Author Manuscript

NIH-PA Author Manuscript

DISCUSSION

DOX-induced cardiomyopathy exhibits different pathogenesis from that of the anemia model

In this study, we reported the second adult zebrafish model of cardiomyopathy that is induced by DOX. Cardiac enlargement occurs at 4 weeks post-DOX injection, which further progressed to decompensational remodeling at later stages, exhibiting hallmarks of cardiomyopathy including activation of fetal gene expression, muscular disarray, and myofibril loss. The enlarged heart and cardiomyocyte hypertrophy is consistent to DOX responses reported in some *in vivo* rodent models and *in vitro* culture system,[24,25,28,34] but is different from other rodent models that report reduced cardiac mass, increased cardiomyocyte atrophy, and dilated cardiomyopathy.[19,20] The discrepancy is likely caused by different doses and/or different treatment protocols of DOX stresses, partially due to different focus on either acute or chronic effects of DOX.[35] At the cellular level, pathogenesis in our DOX model is different from that in the anemia model. First, cardiomyocyte proliferation is not activated in the DOX model, while activated myocyte hyperplasia occurs at all stages of pathogenesis in the anemia model. Given the high regenerative capacity of a zebrafish heart, this was a surprising observation, suggesting that activated cardiomyocyte proliferation is not necessarily a default stress response in a zebrafish heart. Secondly, cardiomyocyte hypertrophy contributes to the enlarged heart in the DOX model at all stages, while cardiomyocyte hypertrophy can be only detected at early stages in the anemia model.[2] Thirdly, significantly activated apoptosis was detected in cardiomyocytes in the DOX model, which had also been reported in other animal models for DOX-induced cardiotoxicity.[27,28] In contrast, oncosis is a more dominant cell death pathway of cardiomyocytes in the anemic model.[2]

It is conceivable that the distinct cellular changes in the DOX model vs. the anemia model are due to different stresses imposed on the heart. Anemia mainly imposes extrinsic stresses on the heart because of the significantly increased demand from the body to compensate for the reduced red blood cell concentration. In addition, hypoxic conditions within the heart might also impose an intrinsic stress. In contrast, DOX inflicts intrinsic damage on cardiomyocytes, most likely due to its disruptive function in mitochondria and consequent activation of oxidative stress in cardiomyocytes.[7,8] The intrinsic nature of this stress is underscored by the observation that DOX induces cellular hypertrophy and apoptosis in cultured cardiomyocytes.

TOR signaling inhibition exerts cardioprotective effects on cardiomyopathies

Taking advantage of the forward genetic screen in zebrafish, we identified *ztor* mutant. Further studies based on the *ztor*$^{+/-}$ fish provided direct genetic evidences to support a cardioprotective function of TOR signaling reduction on cardiomyopathy. This effect has been observed in two types of cardiomyopathies in adult zebrafish of different etiology, prompting an exciting hypothesis, that activated TOR signaling is a common pathological event during cardiomyopathy, which can be intervened for therapeutic benefits.

Our results validated the cardioprotective function of TOR signaling inhibition suggested by pharmacological studies in mice.[10,11,13] However, cardiac-specific knock-out studies of *Mtor* and *raptor* in mouse reported an accelerated heart failure progression upon pressure overload,[36,37] suggesting important functions of TOR signaling in normal cardiac physiology and adaptive cardiac hypertrophy. An important difference between the present study and the mouse studies is the dose of the TOR signaling inhibition. In the mouse studies, *Mtor* signaling was ablated to such a low level that most mice die within 8 weeks.[36,37] In contrast, TOR expression is only reduced to 65% at the protein level in

NIH-PA Author Manuscript

NIH-PA Author Manuscript

NIH-PA Author Manuscript

ztor$^{+/-}$, which allows these fish to survive to adulthood without any noticeable phenotypes. This statement can be better appreciated in the context that extreme starvation will lead to animal death, while regulated caloric restriction protects heart and prolongs their lifespan.[38] Together, our results put forward an important concept, i.e. it is critical to control the dose of TOR signaling inhibition to achieve therapeutic benefits for cardiomyopathies.

TOR has been found to be involved in two structurally and functionally distinct complexes. While TORC1 contains mTOR, mLST8, and raptor and is sensitive to rapamycin, TORC2 contains mTOR, mLST8, rictor, mSIN1, and PRR5 and is insensitive to rapamycin.[39–41] The downstream signaling pathways of the TORC1 complex have been found to regulate protein synthesis, autophagy, and transcription. In contrast, the downstream signaling pathways of the TORC2 complex are implicated in regulating actin cytoskeleton structure.[39–41] As shown in Figure 3I, one-week rapamycin treatment recapitulates the attenuated TORC1 signaling in *ztor*$^{+/-}$ fish, but TORC2 signaling can be either activated or attenuated depending on the treatment protocols. Nevertheless, both rapamycin treatment protocols effectively attenuate cardiac enlargement, suggesting that this anti-hypertrophy function is likely conveyed by the TORC1 rather than the TORC2 complex.

At the cellular level, our data revealed that the cardioprotective effect of TOR signaling inhibition is due to its anti-hypertrophy, anti-apoptosis, and pro-autophagy functions. Although our data derived from primary cardiomyocyte culture support a cell-autonomous function of TOR signaling within cardiomyocytes, it is important to point out that our present approach cannot exclude the possibility that TOR signaling exerts its functions via other cell types in the heart, such as endocardial cells and fibroblasts.

It is of particular interest to note that autophagy is suppressed at later cardiomyopathy stages of the DOX model. Recent studies suggested that the protective autophagy level is reduced at later stages of heart failure, while activated autophagy can exert cardioprotective role by eliminating damaged organelles and/or toxic proteins that contribute to the pathogenesis of cardiomyopathy.[30,42] Therefore, it is tempting to propose that the cardioprotective effect of TOR signaling inhibition might be conveyed by the activated autophagy. Further investigation is warranted to test this hypothesis.

Dynamic activities of TOR along pathogenesis of cardiomyopathies

A unique feature of TOR signaling revealed is that its activity varies significantly at different stages of pathogenesis of cardiomyopathies. In the anemia model, TOR-pS6K signaling is activated concurrently with predominant cardiomyocyte hypertrophy at the early stages, but suppressed at the later stages. In the DOX-induced models, TOR-autophagy signaling of TOR is oppositely regulated during initial acute phase and later cardiomyopathy phase. Furthermore, TOR signaling inhibition exerts opposite effects on DOX-induced acute cardiotoxicity and late onset cardiomyopathy. This stage-dependent effect of TOR signaling explains the seemingly conflicting conclusion on the beneficial effect of TOR activation on DOX-induced acute cardiotoxicity, as reported in murine models,[19,29] and the cardioprotective effect of TOR signaling inhibition on cardiomyopathies. Our results underscore the concept that cardiomyopathy is a progressive disease. It is important to note that distinct signaling events and/or even opposite activities of the same signaling pathway might occur at different stages of pathogenesis.

Together, our data present adult zebrafish as a novel and conserved vertebrate model organism for eliciting molecular mechanism of cardiomyopathies. As exemplified by this study, novel discoveries on dose- and stage-dependent functions of TOR signaling in cardiomyopathies have been made, both of which will be instructive for designing proper therapeutic strategies for DOX-induced cardiomyopathies. Complementing to the existing

NIH-PA Author Manuscript

NIH-PA Author Manuscript

NIH-PA Author Manuscript

rodent models, further investigation utilizing this emerging animal model promises to facilitate our understanding of human cardiomyopathies.

Supplementary Material

Refer to Web version on PubMed Central for supplementary material.

Acknowledgments

We thank Dr. Leonard Zon, Children's Hospital (Boston) for sharing with us the *casper* fish. We appreciate Dr. Daniel Klionsky from University of Michigan for providing us the *Tg(GFP-Lc3)* transgenic fish. We are grateful to Beninio Jomok for his help with zebrafish husbandry.

SOURCES OF FUNDING This study was supported by Mayo Foundation, AHA10GRNT4130009, NIH HL107304 (PI: Dr. Xiaolei Xu), and NIH DA14546 (PI: Dr. Stephen Ekker).

Non-standard Abbreviations and Acronyms

ANF	atrial natriuretic factor
BL	body length
BW	body weight
Brdu	5-bromo-2-deoxyuridine
CM	cardiomyocyte
DOX	doxorubicin
DPF	days post-fertilization
FS	fraction shortening
GBM	gram body mass
PHZ	phenylhydrazine
RBC	red blood cell
RT-PCR	reverse transcription polymerase chain reaction
TOR	target of rapamycin
TUNEL	terminal deoxynucleotidyl transferase dUTP nick end labeling
VA	ventricle area

REFERENCES

1. Shin JT, Fishman MC. From Zebrafish to human: modular medical models. Annu Rev Genomics Hum Genet. 2002; 3:311–340. [PubMed: 12142362]
2. Sun X, Hoage T, Bai P, Ding Y, Chen Z, Zhang R, Huang W, Jahangir A, Paw B, Li YG, Xu X. Cardiac hypertrophy involves both myocyte hypertrophy and hyperplasia in anemic zebrafish. PLoS One. 2009; 4:e6596. [PubMed: 19672293]
3. Paw BH, Davidson AJ, Zhou Y, Li R, Pratt SJ, Lee C, Trede NS, Brownlie A, Donovan A, Liao EC, Ziai JM, Drejer AH, Guo W, Kim CH, Gwynn B, Peters LL, Chernova MN, Alper SL, Zapata A, Wickramasinghe SN, Lee MJ, Lux SE, Fritz A, Postlethwait JH, Zon LI. Cell-specific mitotic defect and dyserythropoiesis associated with erythroid band 3 deficiency. Nat Genet. 2003; 34:59–64. [PubMed: 12669066]
4. Christiansen S, Autschbach R. Doxorubicin in experimental and clinical heart failure. Eur J Cardiothorac Surg. 2006; 30:611–616. [PubMed: 16901709]

NIH-PA Author Manuscript

NIH-PA Author Manuscript

NIH-PA Author Manuscript

5. Robert J. Preclinical assessment of anthracycline cardiotoxicity in laboratory animals: predictiveness and pitfalls. Cell Biol Toxicol. 2007; 23:27–37. [PubMed: 17041747]
6. Yi X, Bekeredjian R, DeFilippis NJ, Siddiquee Z, Fernandez E, Shohet RV. Transcriptional analysis of doxorubicin-induced cardiotoxicity. Am J Physiol Heart Circ Physiol. 2006; 290:H1098–1102. [PubMed: 16243910]
7. Wallace KB. Doxorubicin-induced cardiac mitochondrionopathy. Pharmacol Toxicol. 2003; 93:105–115. [PubMed: 12969434]
8. Simunek T, Sterba M, Popelova O, Adamcova M, Hrdina R, Gersi V. Anthracyclin-induced cardiotoxicity: Overview of studies examing the roles of oxidative stress and free cellular iron. Pharmacological Reports. 2009; 61:154–171. [PubMed: 19307704]
9. Laplante M, Sabatini DM. mTOR signaling at a glance. J Cell Sci. 2009; 122:3589–3594. [PubMed: 19812304]
10. Shioi T, McMullen JR, Tarnavski O, Converso K, Sherwood MC, Manning WJ, Izumo S. Rapamycin attenuates load-induced cardiac hypertrophy in mice. Circulation. 2003; 107:1664–1670. [PubMed: 12668503]
11. McMullen JR, Sherwood MC, Tarnavski O, Zhang L, Dorfman AL, Shioi T, Izumo S. Inhibition of mTOR signaling with rapamycin regresses established cardiac hypertrophy induced by pressure overload. Circulation. 2004; 109:3050–3055. [PubMed: 15184287]
12. Kuzman JA, O'Connell TD, Gerdes AM. Rapamycin prevents thyroid hormone-induced cardiac hypertrophy. Endocrinology. 2007; 148:3477–3484. [PubMed: 17395699]
13. Marin TM, Keith K, Davies B, Conner DA, Guha P, Kalaitzidis D, Wu X, Lauriol J, Wang B, Bauer M, Bronson R, Franchini KG, Neel BG, Kontaridis MI. Rapamycin reverses hypertrophic cardiomyopathy in a mouse model of LEOPARD syndrome-associated PTPN11 mutation. J Clin Invest. 2011; 121:1026–1043. [PubMed: 21339643]
14. Kushwaha SS, Raichlin E, Sheinin Y, Kremers WK, Chandrasekaran K, Brunn GJ, Platt JL. Sirolimus affects cardiomyocytes to reduce left ventricular mass in heart transplant recipients. Eur Heart J. 2008; 29:2742–2750. [PubMed: 18790727]
15. Shen WH, Chen Z, Shi S, Chen H, Zhu W, Penner A, Bu G, Li W, Boyle DW, Rubart M, Field LJ, Abraham R, Liechty EA, Shou W. Cardiac restricted overexpression of kinase-dead mammalian target of rapamycin (mTOR) mutant impairs the mTOR-mediated signaling and cardiac function. J Biol Chem. 2008; 283:13842–13849. [PubMed: 18326485]
16. Sivasubbu S, Balciunas D, Davidson AE, Pickart MA, Hermanson SB, Wangensteen KJ, Wolbrink DC, Ekker SC. Gene-breaking transposon mutagenesis reveals an essential role for histone H2afza in zebrafish larval development. Mech Dev. 2006; 123:513–529. [PubMed: 16859902]
17. Parinov S, Kondrichin I, Korzh V, Emelyanov A. Tol2 transposon-mediated enhancer trap to identify developmentally regulated zebrafish genes in vivo. Dev Dyn. 2004; 231:449–459. [PubMed: 15366023]
18. White RM, Sessa A, Burke C, Bowman T, LeBlanc J, Ceol C, Bourque C, Dovey M, Goessling W, Burns CE, Zon LI. Transparent adult zebrafish as a tool for in vivo transplantation analysis. Cell Stem Cell. 2008; 2:183–189. [PubMed: 18371439]
19. Zhu W, Soonpaa MH, Chen H, Shen W, Payne RM, Liechty EA, Caldwell RL, Shou W, Field LJ. Acute doxorubicin cardiotoxicity is associated with p53-induced inhibition of the mammalian target of rapamycin pathway. Circulation. 2009; 119:99–106. [PubMed: 19103993]
20. Li L, Takemura G, Li Y, Miyata S, Esaki M, Okada H, Kanamori H, Khai NC, Maruyama R, Ogino A, Minatoguchi S, Fujiwara T, Fujiwara H. Preventive effect of erythropoietin on cardiac dysfunction in doxorubicin-induced cardiomyopathy. Circulation. 2006; 113:535–543. [PubMed: 16449733]
21. Sun L, Lien CL, Xu X, Shung KK. In vivo cardiac imaging of adult zebrafish using high frequency ultrasound (45–75 MHz). Ultrasound Med Biol. 2008; 34:31–39. [PubMed: 17825980]
22. Rottbauer W, Saurin AJ, Lickert H, Shen X, Burns CG, Wo ZG, Kemler R, Kingston R, Wu C, Fishman M. Reptin and pontin antagonistically regulate heart growth in zebrafish embryos. Cell. 2002; 111:661–672. [PubMed: 12464178]
23. Lien CL, Schebesta M, Makino S, Weber GJ, Keating MT. Gene expression analysis of zebrafish heart regeneration. PLoS Biol. 2006; 4:e260. [PubMed: 16869712]

NIH-PA Author Manuscript

NIH-PA Author Manuscript

NIH-PA Author Manuscript

24. Merten KE, Jiang Y, Feng W, Kang YJ. Calcineurin activation is not necessary for Doxorubicin-induced hypertrophy in H9c2 embryonic rat cardiac cells: involvement of the phosphoinositide 3-kinase-Akt pathway. J Pharmacol Exp Ther. 2006; 319:934–940. [PubMed: 16926266]
25. Tu VC, Bahl JJ, Chen QM. Signals of oxidant-induced cardiomyocyte hypertrophy: key activation of p70 S6 kinase-1 and phosphoinositide 3-kinase. J Pharmacol Exp Ther. 2002; 300:1101–1110. [PubMed: 11861821]
26. Poss KD, Wilson LG, Keating MT. Heart regeneration in zebrafish. Science. 2002; 298:2188–2190. [PubMed: 12481136]
27. Li K, Sung RY, Huang WZ, Yang M, Pong NH, Lee SM, Chan WY, Zhao H, To MY, Fok TF, Li CK, Wong YO, Ng PC. Thrombopoietin protects against in vitro and in vivo cardiotoxicity induced by doxorubicin. Circulation. 2006; 113:2211–2220. [PubMed: 16651473]
28. Ueno M, Kakinuma Y, Yuhki K, Murakoshi N, Iemitsu M, Miyauchi T, Yamaguchi I. Doxorubicin induces apoptosis by activation of caspase-3 in cultured cardiomyocytes in vitro and rat cardiac ventricles in vivo. J Pharmacol Sci. 2006; 101:151–158. [PubMed: 16766856]
29. Kobayashi S, Volden P, Timm D, Mao K, Xu X, Liang Q. Transcription Factor GATA4 Inhibits Doxorubicin-induced Autophagy and Cardiomyocyte Death. J Biol Chem. 2010; 285:793–804. [PubMed: 19901028]
30. Rothermel BA, Hill JA. Autophagy in load-induced heart disease. Circ Res. 2008; 103:1363–1369. [PubMed: 19059838]
31. Martinet W, Knaapen MW, Kockx MM, De Meyer GR. Autophagy in cardiovascular disease. Trends Mol Med. 2007; 13:482–491. [PubMed: 18029229]
32. He C, Bartholomew CR, Zhou W, Klionsky DJ. Assaying autophagic activity in transgenic GFP-Lc3 and GFP-Gabarap zebrafish embryos. Autophagy. 2009; 5:520–526. [PubMed: 19221467]
33. Bjorkoy G, Lamark T, Brech A, Outzen H, Perander M, Overvatn A, Stenmark H, Johansen T. p62/SQSTM1 forms protein aggregates degraded by autophagy and has a protective effect on huntingtin-induced cell death. J Cell Biol. 2005; 171:603–614. [PubMed: 16286508]
34. Sun X, Zhou Z, Kang YJ. Attenuation of doxorubicin chronic toxicity in metallothioneinoverexpressing transgenic mouse heart. Cancer Res. 2001; 61:3382–3387. [PubMed: 11309296]
35. Hayward R, Hydock DS. Doxorubicin cardiotoxicity in the rat: an in vivo characterization. J Am Assoc Lab Anim Sci. 2007; 46:20–32. [PubMed: 17645292]
36. Zhang D, Contu R, Latronico MV, Zhang JL, Rizzi R, Catalucci D, Miyamoto S, Huang K, Ceci M, Gu Y, Dalton ND, Peterson KL, Guan KL, Brown JH, Chen J, Sonenberg N, Condorelli G. MTORC1 regulates cardiac function and myocyte survival through 4E-BP1 inhibition in mice. J Clin Invest. 2010; 120:2805–2816. [PubMed: 20644257]
37. Shende P, Plaisance I, Morandi C, Pellieux C, Berthonneche C, Zorzato F, Krishnan J, Lerch R, Hall MN, Ruegg MA, Pedrazzini T, Brink M. Cardiac raptor ablation impairs adaptive hypertrophy, alters metabolic gene expression, and causes heart failure in mice. Circulation. 2011; 123:1073–1082. [PubMed: 21357822]
38. Ahmet I, Wan R, Mattson MP, Lakatta EG, Talan M. Cardioprotection by intermittent fasting in rats. Circulation. 2005; 112:3115–3121. [PubMed: 16275865]
39. Inoki K, Guan KL. Complexity of the TOR signaling network. Trends Cell Biol. 2006; 16:206–212. [PubMed: 16516475]
40. Wullschleger S, Loewith R, Hall MN. TOR signaling in growth and metabolism. Cell. 2006; 124:471–484. [PubMed: 16469695]
41. Fingar DC, Blenis J. Target of rapamycin (TOR): an integrator of nutrient and growth factor signals and coordinator of cell growth and cell cycle progression. Oncogene. 2004; 23:3151–3171. [PubMed: 15094765]
42. Gustafsson AB, Gottlieb RA. Recycle or die: the role of autophagy in cardioprotection. J Mol Cell Cardiol. 2008; 44:654–661. [PubMed: 18353358]

NIH-PA Author Manuscript

NIH-PA Author Manuscript

NIH-PA Author Manuscript

Novelty and significance

What is Known?

- Rapamycin is a specific inhibitor of the target of rapamycin (TOR) signaling. It exerts cardioprotective effects on cardiomyopathy; however, genetic studies of functions of TOR signaling in cardiomyopathy have yielded conflicting results.
- The first adult zebrafish model of cardiomyopathy induced by chronic anemia has been generated; however, the value of this new vertebrate model in dissecting underlying signaling pathways remains untested.

What New Information Does This Article Contribute?

- Similar to that in rodents and human, doxorubicin (DOX) induces cardiomyopathy in adult zebrafish.
- Partial reduction of TOR signaling in the zebrafish *tor* heterozygous mutant exerts cardioprotective effects on two cardiomyopathies of distinct etiology, providing the first genetic evidence, indicating that TOR signaling may be a common therapeutic pathway for cardiomyopathies.
- Both dose- and stage- dependent functions of TOR need to be controlled properly when developing TOR-based therapeutics for cardiomyopathies.

Zebrafish is a promising vertebrate model that has the potential to dissect molecular mechanisms of cardiomyopathies via its powerful genetics. Here, we report the generation of the second adult zebrafish model for cardiomyopathy induced by DOX, which validates zebrafish as a conserved novel vertebrate model for genetic studies of cardiomyopathy. Together with the previously reported cardiomyopathy model induced by anemia, we investigated functions of TOR signaling in these two types of cardiomyopathies. Despite different etiology and pathogenesis, short-term treatment of rapamycin effectively attenuated cardiac enlargement in both models. However, this anti-hypertrophy effect was stage-dependent, because of dynamic activities of TOR along the pathogenesis of these models. We assessed the long-term effect of TOR inhibition using a zebrafish *tor* mutant that we identified from an insertional mutagenesis screen. We found that long-term TOR signaling inhibition improved cardiac function and fish survival rate, providing the first genetic evidence to support a cardioprotective function of TOR inhibition. Taken together, our data suggest that TOR is a common therapeutic pathway that can be leveraged to develop therapeutics for cardiomyopathies of distinct etiology. Importantly, the dose- and stage- dependent functions may be instructive to developing TOR-based therapeutic strategies.

NIH-PA Author Manuscript

NIH-PA Author Manuscript

NIH-PA Author Manuscript

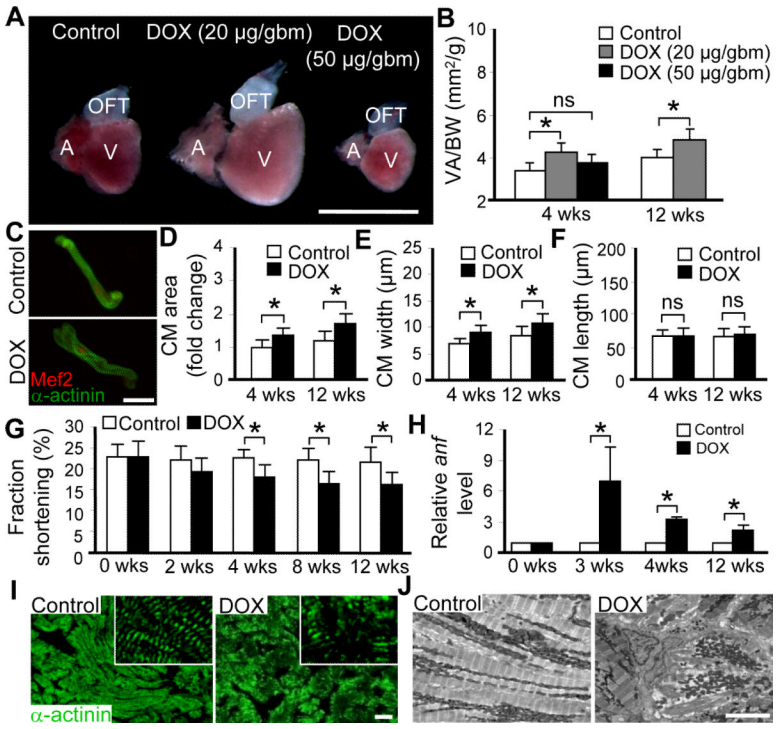

Figure 1. DOX-induced cardiomyopathy in zebrafish

A, Representative images of dissected hearts from *casper* fish at 4 weeks post-injection with low (20 μg/gbm) or high (50 μg/gbm) dose of doxorubicin (DOX). Scale bar=1 mm. B, Quantification of the ventricle area to body weight index (VA/BW) showed heart enlargement at both 4 and 12 weeks post-DOX (20 μg/gbm) injection. C, Representative images of single cardiomyocyte (CM) dissociated from fish hearts at 12 weeks post-DOX (20 μg/gbm) injection. CMs were co-stained with α-actinin and Mef2. Scale bar=20 μm. D, Quantification of CM area to show that CM size was increased in fish hearts at both 4 and 12 weeks post-DOX (20 μg/gbm) injection, which could be explained by increased CM width (E), but not CM length (F). G, Time courses of fraction shortening (FS) measuring using *casper;Tg(cmlc2:nuDsRed)* fish after 20 μg/gbm DOX injection. Significantly decreased FS was detected at 4 weeks and thereafter post-DOX injection. H, Quantitative RT-PCR showing re-activated expression of *atrial natriuretic factor* (*anf*) in 20 μg/gbm DOX-induced cardiac remodeling process. I, α-actinin antibody staining to show muscular disarray at 12 weeks post 20 μg/gbm DOX injection. Insets are images of higher magnification. Scale bar=20 μm. J, Transmission electron microscopy (TEM) verified muscular disarray and myofibril loss in fish hearts at 6 months post 20 μg/gbm DOX injection. Scale bar=5 μm. V, ventricle; A, atrium; OFT, outflow tract. *P<0.05.

NIH-PA Author Manuscript

NIH-PA Author Manuscript

NIH-PA Author Manuscript

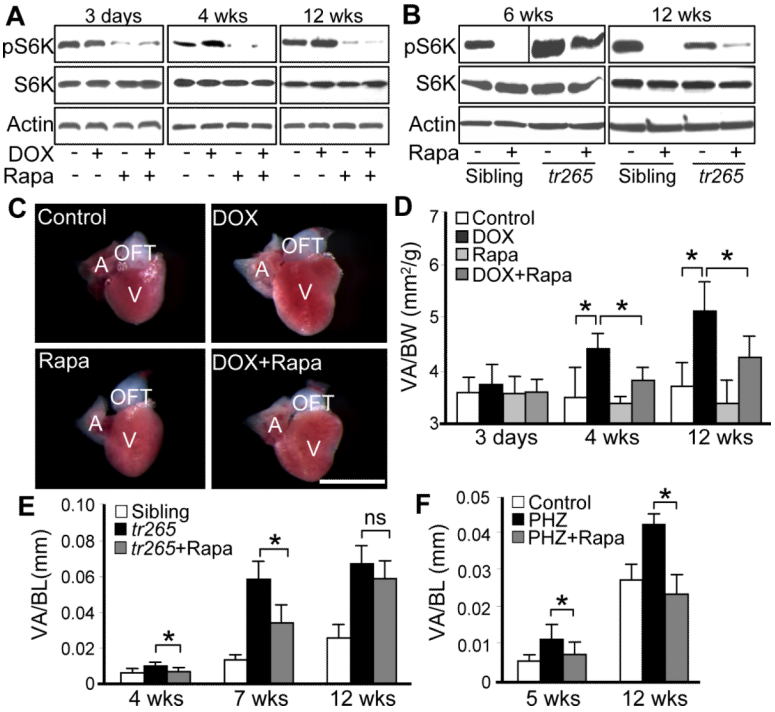

Figure 2. Effects of rapamycin on cardiac enlargement induced by either DOX or anemia

A, TOR activity dynamics in fish hearts injected with DOX (20 μg/gbm) with or without rapamycin (0.2 μmol/L) treatment. B, TOR activity in fish hearts dissected from *tr265* sibling and *tr265* homozygous mutant with or without rapamycin (0.4 μmol/L) treatment. C, Representative images of dissected fish hearts at week 4 post-DOX (20 μg/gbm) injection with or without rapamycin (0.2 μmol/L) treatment. Scale bar=1 mm. D, Quantification of ventricle area to body weight index (VA/BW) at different time points post-DOX injection with or without rapamycin (0.2 μmol/L) treatment. E, Quantification of VA/BW index at different ages of *tr265* fish compared to sibling with or without rapamycin (0.4 μmol/L) treatment. F, Quantification of VA/BW index to show one-week rapamycin (0.4 μmol/L) treatment attenuates phenylhydrazine (PHZ) induced heart enlargement at both 5 weeks and 12 weeks old fish. *P<0.05. ns, not significant. V, ventricle; A, atrium; OFT, outflow tract.

NIH-PA Author Manuscript

NIH-PA Author Manuscript

NIH-PA Author Manuscript

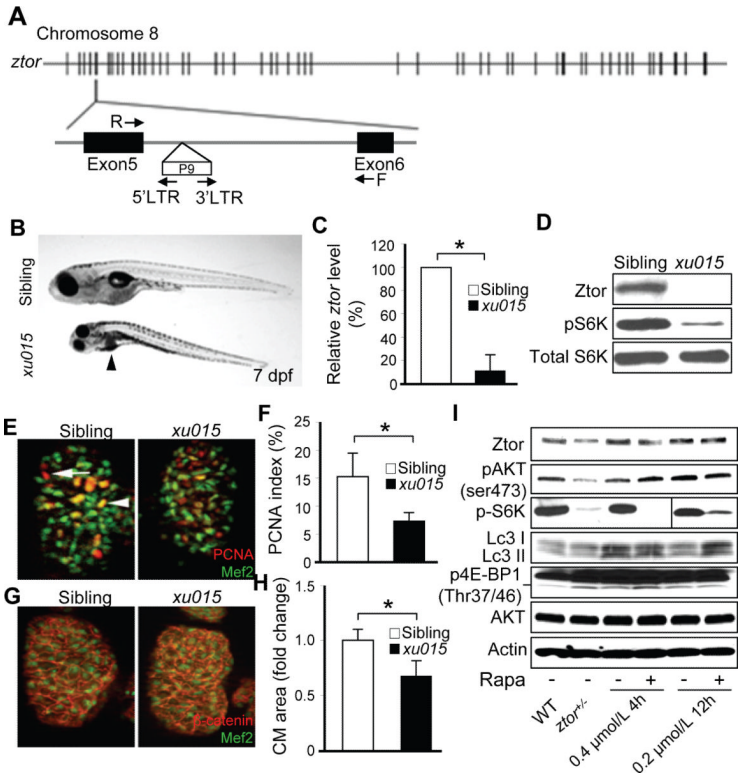

Figure 3. Isolation of a zebrafish target of rapamycin hypomorphic mutant: *ztorxu015*

A, A P9 insertion was inserted within the 5th intron of the *zebrafish target of rapamycin (ztor)* gene at chromosome 8 in the *ztorxu015* mutant. Locations of the primers used in LM-PCR and genotyping are indicated by arrows. B, The homozygous *ztorxu015* mutant *(ztor−/−)* embryos appeared to be smaller compared to their normal siblings and displayed dark liver phenotypes at 7 days post-fertilization (dpf). Arrowheads indicate location of the liver. C, Quantificative RT-PCR revealed that the mRNA level of *ztor* was reduced by about 90% in the *ztor−/−* compared to that in normal siblings at 7 dpf. D, Western blot analysis confirmed a dramatic reduction of Ztor protein in the *ztor−/−* mutant at 7 dpf. In addition, phosphor-ribosomal S6K was also dramatically reduced, while the total ribosomal S6K level remained unchanged in the *ztor−/−* mutant. E, Representative images of dissected fish hearts at 7 dpf after co-immunostained with Mef2 (green) to label CMs and PCNA (red) to label proliferative cells. Scale bar=10 μm. Arrowhead indicates a proliferating CM. Arrow indicates a proliferating non-CM. F, Quantification of CM proliferation index represented in (E). G, Representative images of dissected fish hearts at 7 dpf after co-immunostained with Mef2 (green) and β-catenin (red) to define borders of CMs. H, Quantification of CM cell size represented in (G). I, Expression levels of total Ztor protein and its downstream branches of TORC1 and TORC2 in 6-month old *ztorxu015* heterozygous fish (*ztor+/−*) compared to that in wild type siblings treated with or without rapamycin (0.4 μmol/L 4 h daily or 0.2 μmol/L 12 h daily for consecutive 7 days). p4E-BP1 level is indicated by the lower band. *P<0.05.

NIH-PA Author Manuscript

NIH-PA Author Manuscript

NIH-PA Author Manuscript

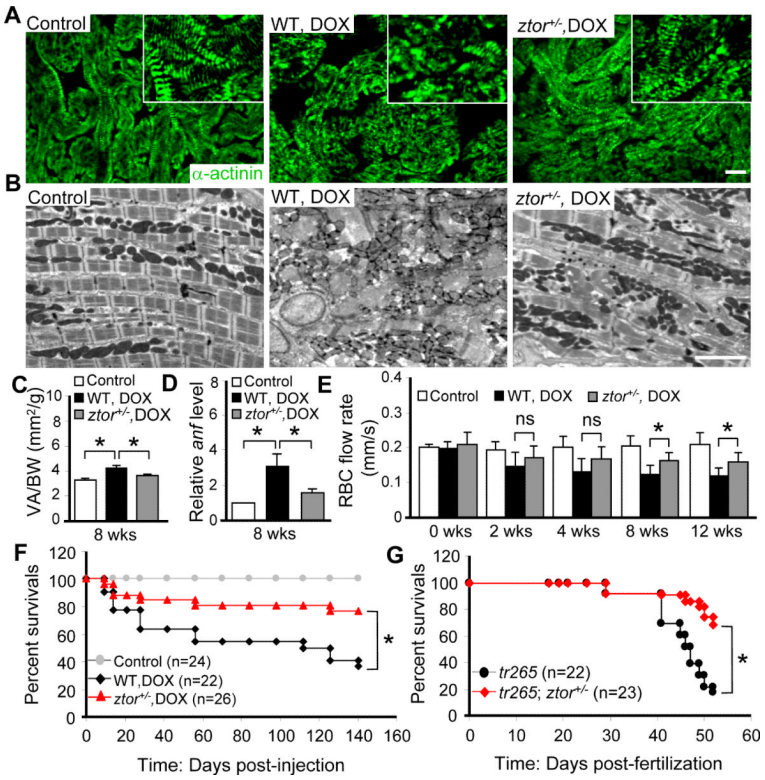

Figure 4. TOR haploinsufficiency attenuates DOX or anemia-induced cardiomyopathy

A, α-actinin antibody staining showing attenuated muscular disarray detected in the *ztor*+/− fish ventricle compared to that in wild type control at week 12 after 20 ug/gbm DOX injection. Insets are images of higher magnification. Scale bar=20 μm. B, Transmission electron microscopy (TEM) showing attenuated muscular disarray and myofibril loss detected in the *ztor*+/− fish ventricle compared to that in wild type control at 6 months after 20 μg/gbm DOX injection. Scale bar=5 μm. C, Quantification data to show *ztor*+/− fish had significantly attenuated ventricular enlargement compared to that in wild type control at week 8 after 20 μg/gbm DOX injection. D, Evaluation of fetal gene expression by quantitative RT-PCR. *anf* expression was reduced in the *ztor*+/− heart compared to that in wild type control at week 12 after 20 μg/gbm DOX injection. E, Evaluation of cardiac function by quantifying the red blood cell (RBC) flow rate. The *ztor*+/− fish exhibited improved RBC flow rate compared to that in wild type control treated with 20 μg/gbm DOX since week 8. F, Kaplan-Meier survival curves of the *ztor*+/− and wild type fish treated with 20 μg/gbm DOX vs. untreated wild type control. G, Kaplan-Meier survival curves of the *tr265; ztor*+/− fish compared to that in the *tr265*. *P<0.05. ns, not significant.

NIH-PA Author Manuscript

NIH-PA Author Manuscript

NIH-PA Author Manuscript

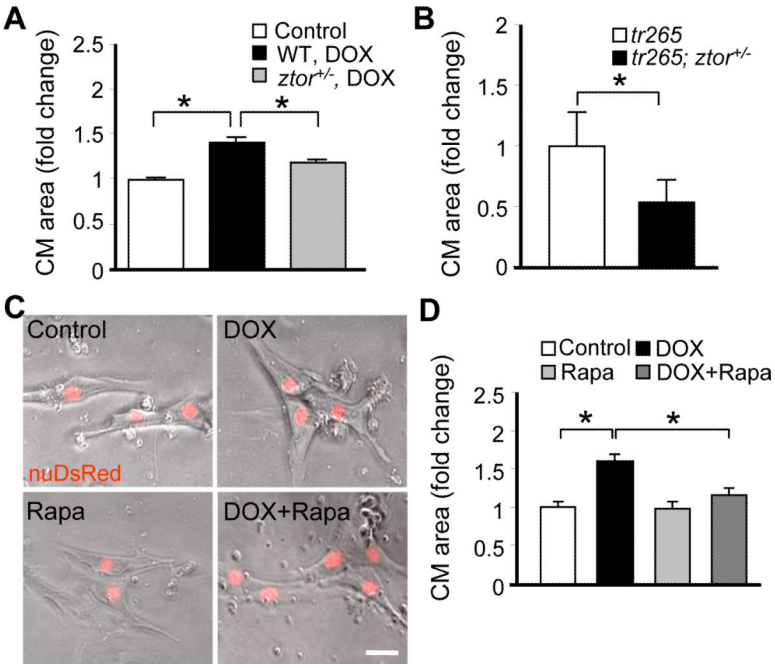

Figure 5. TOR signaling inhibition attenuates cardiomyocyte hypertrophy

A, Quantification data to show *ztor*+/− fish had significantly attenuated CM cell size compared to that in wild type control at week 8 after 20 μg/gbm DOX injection. B, Quantification data to show *tr265; ztor*+/− fish had significantly attenuated CM cell size compared to that in *tr265* fish at 6 weeks old age. C, Representative images of primary cultured CMs treated with 2 h of DOX (5 μmol/L) with or without rapamycin (0.2 μmol/L) co-treatment. Scale bar=20 μm. D, Quantification of CM cell size to show that DOX-induced cellular hypertrophy was attenuated by rapamycin co-treatment. *P<0.05.

NIH-PA Author Manuscript
NIH-PA Author Manuscript
NIH-PA Author Manuscript

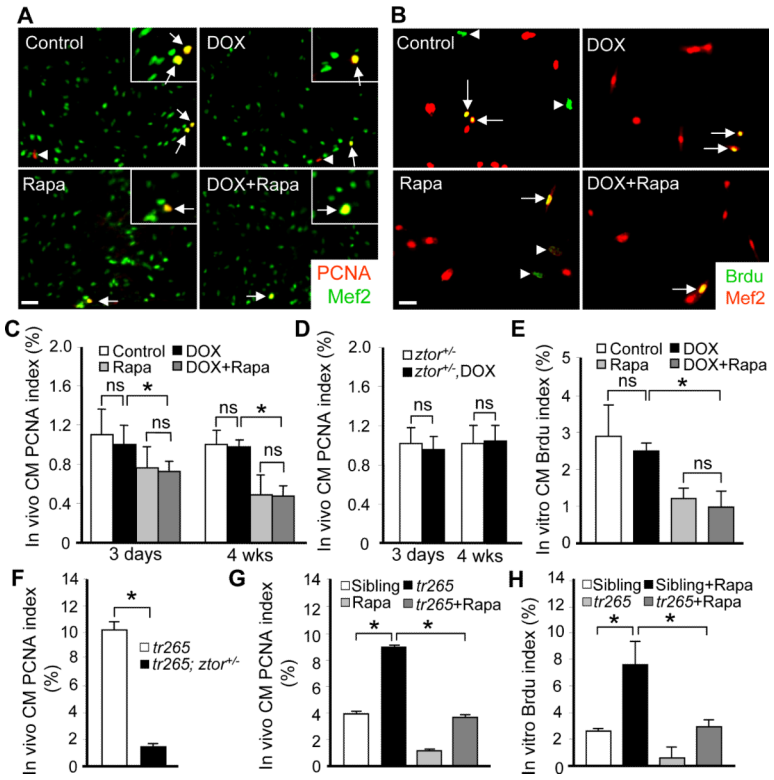

Figure 6. Effects of DOX and TOR inhibition on myocyte proliferation

A, Merged images of sectioned fish ventricles co-stained with PCNA (red) and Mef2 (green) at 4 weeks after 20 ug/gbm DOX injection with or without rapamycin (0.2 μmol/L) treatment. Insets are images of higher magnification. Arrows: PCNA+/Mef2+ cells; Arrowheads: PCNA+/Mef2-cells. Scale bar=20 μm. B, Merged images of primary cultured CMs co-stained with BrdU (green) and Mef2 (red) after 2 h of DOX treatment (5 μmol/L) with or without rapamycin (0.2 μmol/L) co-treatment. Scale bar=20 μm. Arrows: BrdU+/Mef2+ cells; arrowheads: BrdU+/Mef2-cells. C, Quantification of the PCNA index in fish heart represented in (A). D, Quantification of PCNA index in the sectioned ventricles of *ztor* +/− fish with or without DOX injection at both 3 days and 4 weeks time points. E, Quantification of the BrdU index from primary cultured CMs represented in (B). F, Evaluation of hyperplasia by quantifying CM PCNA index in sectioned hearts represented in *tr265*; *ztor*+/− compared to that in *tr265*. G, Quantification of PCNA index in *tr265* fish with or without rapamycin (0.4 μmol/L) treatment at 6 weeks old age. H, Quantification of primary cultured Brdu index in *tr265* fish with or without rapamycin (0.4 μmol/L) treatment *in vitro*. *P<0.05. ns, not significant.

NIH-PA Author Manuscript

NIH-PA Author Manuscript

NIH-PA Author Manuscript

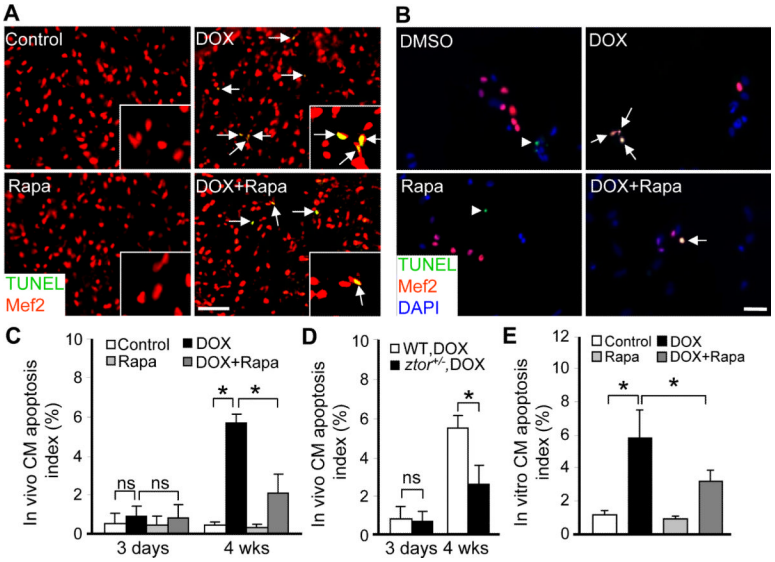

Figure 7. Effects of TOR inhibition on cardiomyocyte apoptosis

A, Merged images of sectioned fish ventricles co-stained with TUNEL (green) and Mef2 (red) at 4 weeks after 20 ug/gbm DOX injection with or without rapamycin (0.2 μmol/L) treatment. Insets are images of higher magnification. Arrows: Mef2+/TUNEL+ cells. Scale bar=20 μm. B, Merged images of primary cultured CMs co-stained with TUNEL (green), Mef2 (red) and DAPI (blue) after 2 h of DOX (5 μmol/L) treatment with or without rapamycin (0.2 μmol/L) co-treatment. Arrows: TUNEL+/Mef2+ cells; arrowheads: TUNEL +/Mef2-cells. Scale bar=20 μm. C, Quantification of apoptotic cells in sectioned ventricles to show dramatically increased apoptosis at 4 weeks, but not 3 days after 20 μg/gbm DOX injection, and rapamycin attenuates 20 μg/gbm DOX-induced apoptosis significantly. D, Quantification of apoptotic cells in sectioned ventricles to show significantly reduced apoptosis was observed in *ztor*+/− fish compared to that in wild type fish at 4 weeks, but not 3 days after 20 μg/gbm DOX injection. E, Quantification of the TUNEL index from (B) showed that 5 μmol/L DOX induced significant apoptosis in primary cultured CMs and that rapamycin was able to inhibit DOX-induced apoptosis *in vitro*. *P<0.05. ns, not significant.

NIH-PA Author Manuscript

NIH-PA Author Manuscript

NIH-PA Author Manuscript

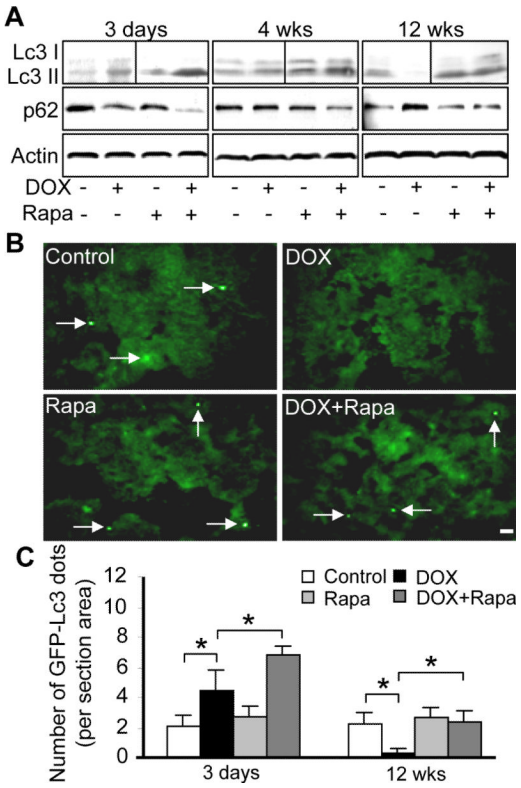

Figure 8. Opposite autophagy activities at early and later stages post-DOX injection

A, Shown are western blotting to assess the autophagy activity dynamics in fish hearts injected with DOX (20 μg/gbm) with or without rapamycin (0.2 μmol/L) treatment, as indicated by both Lc3 conversion and p62 degradation. B, Represented images of sectioned ventricles of *Tg(GFP-Lc3)* fish at 12 weeks after 20 μg/gbm DOX injection with or without rapamycin (0.2 μmol/L) treatment. Arrows: Lc3 aggregating dots formed during autophagy. C, Quantification of GFP-Lc3 aggregation dots in fish ventricles at 3 days and 12 weeks after 20 μg/gbm DOX injection with or without rapamycin (0.2 μmol/L) treatment. *P<0.05.